*Biochimica et Biophysica Acta*, 347 (1974) 340–358


BBA 46751

# MITOCHONDRIAL FUNCTIONS UNDER HYPOXIC CONDITIONS

## THE STEADY STATES OF CYTOCHROME *c* REDUCTION AND OF ENERGY METABOLISM

TUKASA SUGANO*, NOZOMU OSHINO and BRITTON CHANCE

*Johnson Research Foundation, School of Medicine, University of Pennsylvania, Philadelphia, Pa. 19174 (U.S.A.)*

(Received December 7th, 1973)

SUMMARY

1. The effect of low oxygen concentration on the oxidation–reduction states of cytochrome *c* and of pyridine nucleotide, on $Ca^{2+}$ uptake, on the energy-linked reduction of pyridine nucleotide by succinate, and on the rate of oxygen consumption have been examined under various metabolic conditions, using pigeon heart mitochondria.

2. The oxygen concentration required to provide half-maximal reduction of cytochrome *c* ($p50_c$) ranges from 0.27 to 0.03 $\mu$M (0.2–0.02 Torr) depending upon the metabolic activity. There is a linear increase of the $p50_c$ value with increasing respiratory rate.

3. The fraction of the normoxic respiration that is observed at $p50_c$ is 70–90 % under State 4 conditions, but is 30 % under State 3 conditions.

4. The oxygen requirement for half-maximal reduction of pyridine nucleotide ($p50_{PN}$) varies less than $p50_c$, being 0.08 $\mu$M in State 3 and 0.06 $\mu$M in the uncoupled state.

5. The ability of the mitochondria to exhibit an energy-linked reduction of pyridine nucleotide by succinate disappears at an oxygen concentration of 0.09 $\mu$M (0.06 Torr). Below this oxygen concentration, endogenous $Ca^{2+}$ begins to be released from the mitochondria. Thus, the critical oxygen concentration for bioenergetic function of mitochondria corresponds approximately to 50 % reduction of pyridine nucleotide ($p50_{PN}$).

## INTRODUCTION

On a physiological basis, tissue oxygen requirements have been evaluated largely in terms of the arterial and venous oxygen concentrations and the difference between these two quantities as measured across a particular organ. For such measure-

* Permanent address: College of Agriculture, University of Osaka Prefecture, Sakai-city, Osaka, Japan.

ments hemoglobin operates satisfactorily as an extracellular oxygen indicator in the range of $pO_2$ from 60 to 4 Torr, where tissue respiration begins to decrease [1–3]. On the supposition that the affinity of the cytochrome oxidase system was not much less than that of hemoglobin, and considering values in the neighborhood of 1 $\mu$M as determined by platinum microelectrode measurements [4] the gradient of oxygen concentration from the blood to the tissue was considered to be on the order of 10-fold. More recent measurements of the p50 of cytochrome oxidase in the mitochondria [2, 5] now indicate considerably lower values which have been confirmed by Lübbers as well [6]. Thus, the tissue oxygen gradient from capillary to mitochondrion can be as high as 1000-fold, and hemoglobin can no longer be considered to be a useful reference point for calculating the intracellular oxygen concentration. Therefore, new intracellular oxygen indicators must be developed and calibrated.

One possibility is to use a pigment which binds tissue oxygen, such as myoglobin in cardiac and skeletal tissue or hemoglobin in yeast cells [7]. Both these pigments can be extracted from the cell, purified, and their in vitro oxygen affinity precisely calibrated. On the assumption that the in vitro values apply in vivo, they may be used as intracellular oxygen indicators.

The mitochondria themselves are highly pigmented and contain cytochromes, flavoproteins, and quinones that can be detected spectrophotometrically, flavoproteins and pyridine nucleotides that can be detected fluorimetrically, and iron–sulfur proteins and copper components that can be detected by electron paramagnetic resonance. The oxidation–reduction states of all these components are affected by oxygen utilization in the mitochondria and in this sense they are paragons of oxygen determination in situ. Since mitochondrial energy production associated with cellular respiration is controlled first by the combination of utilizable substrates, secondly by the energy requirements for cellular function, and thirdly by the intracellular oxygen concentration, the oxygen dependence of the redox states of these pigments is affected by many factors. Nevertheless, they provide useful tools in combination with myoglobin or yeast hemoglobin signals, for the understanding and investigation of the intracellular oxygen tension, cell bioenergetics, and metabolism.

A definition of critical oxygen concentration [8, 9] is useful in these studies; it may be considered to be the intracellular oxygen concentration at which cellular oxygen utilization begins to decrease. From the kinetic point of view, this is the oxygen concentration at which the mitochondrial respiration rate makes a transition from zero-order to first-order kinetics with respect to oxygen concentration [5]. These oxygen concentrations also affect the redox states of the various components of the mitochondrial respiratory chain; those considered in detail here are cytochrome *c* measured spectrophotometrically and reduced pyridine nucleotide (NADH) measured fluorimetrically.

Of somewhat more interest to biochemical and physiological regulation is the oxygen concentration, or the degree of cytochrome or pyridine nucleotide reduction, at which ATP formation is impaired; these may be termed the critical oxygen tension or degree of pigment reduction, respectively, for energy coupling. This idea may be extended to identify the degree of pigment reduction associated with the failure of a particular biological function. To this point, we have attempted to identify the critical pyridine nucleotide reduction corresponding to the cessation of the electrocorticogram on the brain of the anesthetized rat, the "CPNR" [10]. Which of these various

terms will be most useful depends upon the application in mind; however, the critical oxygen concentrations for electron transport and energy coupling, as indicated by the degree of reduction of cytochrome *c* and pyridine nucleotide, will be reported here. Their application to in situ or in vivo problems will be discussed.

## MATERIALS AND METHODS

### *Oxygen assay*

*Photobacterium phosphoreum* was obtained through the courtesy of Dr F. H. Johnson of Princeton University. The assay procedure for oxygen was as described previously [11, 12] except that the cuvette was a cylinder with a diameter of 2.5 cm and a height of 10 cm, and was equipped with an inlet and outlet for the gas stream.

In order to maintain stable luminescence of the bacteria, the reaction mixture must be hyperosmotic [12]. Thus the reaction mixture in a total volume of 30 ml contained 0.5 M mannitol, 0.1 M potassium phosphate, pH 7.2, 0.02 M KCl, and 0.01 M glucose; this medium was designated "high phosphate". When desired, it was supplemented with respiratory substrates, $MgCl_2$ (2 mM), an ATP-generating system, an ADP-generating system, or other chemicals. In the medium designated as "high chloride", the concentrations of potassium phosphate and KCl were altered to 0.01 M and 0.1 M, respectively. Although the results presented in this paper were obtained primarily with "high phosphate" medium, the "high chloride" medium provided almost identical results, unless otherwise stated.

The ultimate standards used in calibrating the bacterial luminescence were solutions of oxygen equilibrated with air, or pure oxygen at 1 atm, at 25 °C. Aliquots of these standardized solutions were added to the reaction mixture of 120 ml under an Ar stream. The responses of luminescence intensity to varying oxygen concentrations could be monitored on the assumption that a negligible portion of the added oxygen is utilized in the interval between addition and registration [12]. This is quite true for dilute suspensions of bacteria, and the calibration curve of Fig. 1 was obtained under these conditions. In cases where the respiration rate is higher, as for example in mitochondrial suspensions, this calibration method cannot be applied and therefore the already calibrated bacterial luminescence was used as a secondary standard for oxygen concentration.

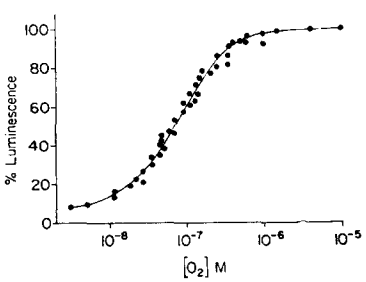


Fig. 1. Relation between luminescence intensity and oxygen concentration. *Ph. phosphoreum* (100 mg wet weight/120 ml) was suspended in hyperosmotic medium (either "high chloride" or "high phosphate"). Changes in luminescence intensity corresponding to known concentrations of oxygen were measured at 475 nm as described in ref. 12. This curve was used as a calibration curve in the experiments which follow.

Similarly, the oxygen profiles for the redox state of cytochrome *c* may be used as a secondary standard, provided that flux conditions have been duplicated in the calibration experiment and when oxygen concentrations have been determined for the redox state of cytochrome *c* in vitro. This method is especially useful under conditions where the bacterial luminescence may interfere with the measurement of pyridine nucleotide fluorescence or aequorin luminescence (see below).

Although the calibration curve of Fig. 1, obtained with the present bacterial strain differs from that obtained with a previous strain [12], the validity of the calibration was confirmed by the fact that the oxygen affinity of purified yeast hemoglobin as determined by both strains was identical ($2 \cdot 10^{-8}$ M).

*Titration of the redox state of cytochrome c with oxygen*

Appropriate concentrations of pigeon heart mitochondria (0.5 mg per ml) and *Ph. phosphoreum* (1–2 mg wet weight/ml) were suspended in either "high phosphate" or "high chloride" medium. The changes in the redox state of cytochrome *c* in response to changes in oxygen concentration were followed at 550–540 nm with simultaneous measurement of bacterial luminescence at 475 nm in a time-sharing spectrophotometer [13]. Interference filters appropriate to these wavelengths were contained in a small disk which was rotated at 60 Hz, thus providing one illumination of the sample every 16 ms. Appropriate electrical gates measured the difference between the signals corresponding to the wavelength pairs of interest, and strip chart recorders presented these differences as a function of time, usually at high sensitivity.

$p50_c$ was defined as the oxygen concentration required for half-maximal reduction of cytochrome *c*. For calibration, the anaerobic steady state of cytochrome *c* reduction observed under Ar gas flow was assumed to be the maximal level of reduction of the cytochrome. The maximum oxidation level of cytochrome *c* in the presence of various substrates was assumed to be that observed with a gas flow of 100 % $O_2$, although cytochrome *c* was not completely oxidized under such conditions. When "high phosphate" and "high chloride" media were used, the steady states of cytochrome *c* reduction were below 10 % with various substrates. In the "standard" medium, this value increased to 20–25 % reduction with succinate plus glutamate, and was 6–8 % with glutamate only.

*Redox state of mitochondrial pyridine nucleotides*

The redox state of mitochondrial pyridine nucleotides was measured fluorimetrically with excitation at 360 nm and emission measurement at 450 nm. Since bacterial luminescence occurs in the same wavelength region as pyridine nucleotide fluorescence [12], the oxidation–reduction state of cytochrome *c*, previously calibrated by bacterial luminescence, was used to calibrate the oxygen concentration in the measurement of pyridine nucleotide reduction. Suitable controls indicated that the bacteria themselves did not alter the apparent oxygen affinity of the mitochondria [7, 12]. It should be noted, however, that in such experiments the "standard medium" (0.225 M mannitol, 0.075 M sucrose, 0.02 M morpholinopropane sulfonate, pH 7.2, 0.002 M KCl, 0.2 mM EDTA, and appropriate concentrations of substrates) was used, on the assumption that the apparent oxygen affinity of cytochrome *c* was not significantly different in the standard medium from that in the hyperosmotic media.

*Assay for $Ca^{2+}$ efflux from mitochondria*

The reaction mixture was the same as that described for the measurement of pyridine nucleotide reduction, except that EDTA was omitted and 0.2 mM $MgCl_2$ and 2 mM potassium phosphate was added. The jellyfish protein, aequorin, also kindly donated by Dr F. H. Johnson, exhibits intense bioluminescence when it combines with $Ca^{2+}$ [14]. The aequorin luminescence intensity was measured at 475 nm, using the same detection system as described above for bacterial luminescence. The oxygen concentrations were estimated from the redox state of cytochrome *c*, which was measured simultaneously, having been previously calibrated with oxygen by bacterial luminescence. An aequorin solution saturated with $(NH_4)_2SO_4$ containing 0.01 M EDTA was added to the reaction mixture with a dilution factor of $6 : 1 \cdot 10^5$, the final concentration of aequorin being approx. 2 nM.

*Measurement of the respiratory rate*

The rate of aerobic respiration was measured using the Clark-type oxygen electrode in the range of oxygen concentrations above 10 $\mu$M, and the measured rates were taken to be the maximal rates of oxygen consumption in the various systems. At oxygen concentrations below 1 $\mu$M, the rates of oxygen consumption were estimated from the change of intensity of bacterial luminescence. The reaction mixture (either "high phosphate" or "high chloride" medium) was first bubbled with Ar gas for 7–10 min and then 0.2 mg wet weight per ml of *Ph. phosphoreum* was added under the Ar gas stream. Bacterial respiration consumed the remaining oxygen within 5 min, and the time course of the luminescence change was recorded. Pigeon heart mitochondria (0.2 mg protein/ml) were then added to the anaerobic reaction mixture together with 0.025 ml of oxygen-saturated water, which provided a final concentration of approx. 1 $\mu$M oxygen. After a few seconds of stirring, the time course of the luminescence change was recorded under the Ar gas stream without stirring. The kinetic recordings of the disappearance of luminescence thus obtained with bacteria alone and with bacteria plus mitochondria were converted to the time course of oxygen disappearance using a calibration curve, and plotted as a function of time in semi-logarithmic coordinates. The rate of mitochondrial respiration at a given oxygen concentration was estimated by subtracting the bacterial respiration from the overall respiration rate at that oxygen concentration.

All the measurements described in this paper were carried out at room temperature (23–25 °C).

*Other procedures*

Pigeon heart mitochondria were prepared according to the method of Chance and Hagihara [15]. Pyruvate kinase (14 I.U./ml) was used with 3 mM phosphoenolpyruvate as an ATP-generating system. For an ADP-generating system, hexokinase (10 I.U. per ml) was used with 10 mM glucose and 2 mM potassium phosphate. Protein was determined by the Biuret method using bovine serum albumin as a standard.

*Materials*

Hexokinase and pyruvate kinase were purchased from Sigma Chemical Co., St. Louis, Mo. Ultra-pure argon (99.999 % pure) was obtained from Matheson Gas Products, Gloucester, Mass.

RESULTS

*Effect of hyperosmolarity on mitochondrial respiration*

The effects of "high phosphate" and "high chloride" media on mitochondrial respiration were compared with that of the "standard" medium. In State 3, the oxygen uptake of the freshly prepared pigeon heart mitochondria is identical in all media. Respiratory rates in State 4, on the other hand, are faster in "high chloride" medium and slower in "high phosphate" medium than in the standard medium. The ADP/O ratio and the respiratory control ratio, which are shown in Fig. 2, are slightly lower in both hyperosmotic media than in the standard medium. These characteristics of respiration were not altered significantly by 30 min incubation with each medium at room temperature.

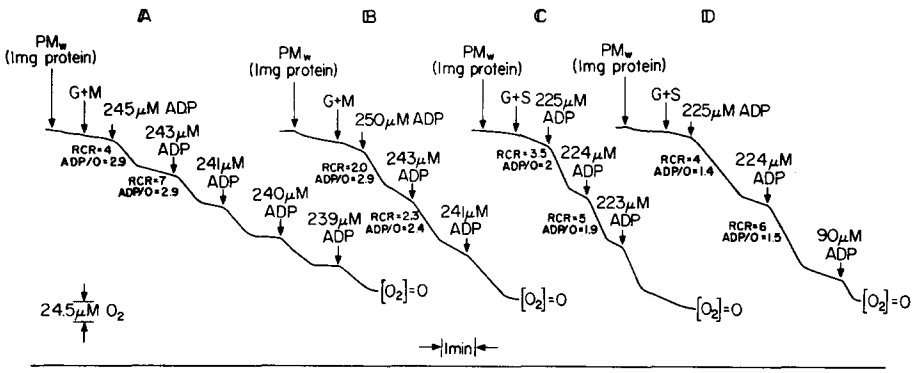


Fig. 2. The effect of hyperosmolarity on mitochondrial respiration. Pigeon heart mitochondria ($PM_w$), 1 mg of protein per ml, were suspended in 2 ml of "standard" medium in Traces A and C, "high chloride" medium in Trace B, and "high phosphate" medium in Trace D. The oxygen concentration was measured by the Clark-type oxygen electrode. G, glutamate, 6 mM; S, succinate, 6 mM; RCR, respiratory control ratio. 24 °C.

*Oxygen dependence of the redox state of mitochondrial cytochrome c*

In isolated mitochondria, the redox state of cytochrome *c* was assumed to have a fixed relationship to the oxygen concentration because this cytochrome is not directly coupled to the phosphorylation system. The relationship between the redox state of cytochrome *c* and the intensity of bacterial luminescence as an oxygen indicator is shown in Fig. 3. Both the redox state of cytochrome *c* and the oxygen concentration are altered by decreasing the $O_2$ concentration in the gas phase in a stepwise fashion and allowing sufficient time for the establishment of a steady state. Although the pigeon heart mitochondria swelled slightly during this particular experiment, the relationship between the redox state of cytochrome *c* and the oxygen concentration in the medium is reproducible in the oxygenation and deoxygenation processes.

Fig. 4 shows the relationships between the percent oxidation of cytochrome *c* and the oxygen concentration in States 3 and 4 and in the antimycin A-inhibited state. It is apparent that the oxygen concentration producing half-maximal reduction of cytochrome *c* ($p50_c$) varies, depending upon the metabolic state; $p50_c$ is as large as 0.25 $\mu$M in State 3 and falls to 0.04 $\mu$M in the antimycin A-inhibited state. With

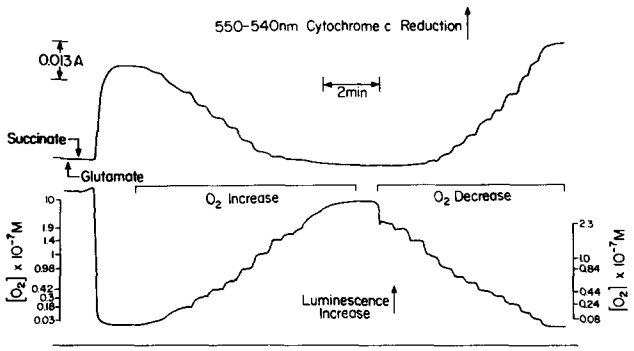


Fig. 3. Redox state of cytochrome *c* corresponding to various oxygen concentrations. 50 mg wet weight of *Ph. phosphoreum* and 15 mg of pigeon heart mitochondrial protein suspended in 30 ml of a reaction mixture containing 0.5 M mannitol, 0.1 M KCl, 0.01 M $K_2PO_4$ (pH 7.2), 0.2 mM EDTA and 15 $\mu$g antimycin A. Succinate and glutamate were added at 6 mM.

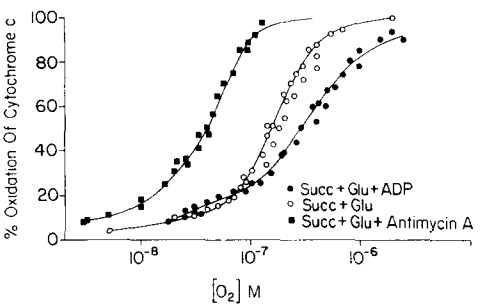


Fig. 4. The relation between the redox state of cytochrome *c* and the oxygen concentration in State 3, State 4, and antimycin A-inhibited conditions. 50 mg wet weight of *Ph. phosphoreum* and 15 mg of protein from pigeon heart mitochondria were suspended in 30 ml of a reaction medium containing 0.5 M mannitol, 0.02 M KCl, 0.1 M $K_2PO_4$ (pH 7.2) and 0.2 mM EDTA. The State 3 condition was maintained with 10 mM glucose, 2 mM $MgCl_2$, 300 I.U. of hexokinase and 0.5 mM ADP, which was added after anaerobiosis was established. The figure represents the results of five separate measurements of each metabolic condition.

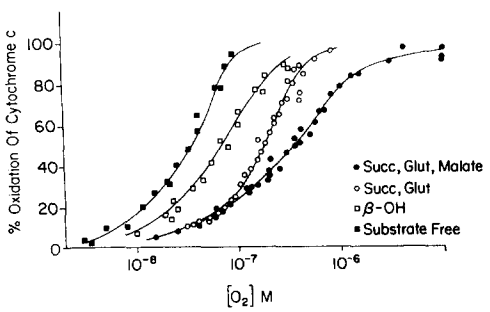


Fig. 5. Effect of substrate on the relation between the redox state of cytochrome *c* and the oxygen concentration. The reaction conditions were as described for Fig. 4, except that the substrate was changed as indicated.

succinate plus glutamate as substrates, $p50_c$ is lower in the presence of ATP than in the absence of ATP.

Changes in the substrate also cause changes in $p50_c$ values, as shown in Fig. 5. $p50_c$ observed with endogenous substrate is identical to that in the antimycin A-inhibited state. Increases in malonate concentration in the presence of succinate plus glutamate result in a progressive decrease of $p50_c$ towards the value observed with glutamate alone (data not shown here). In most cases, the slopes are steeper in State 4 than in State 3 (cf. Fig. 11 also). Differences in the shape and slope of the curves may reflect the redox state of other cytochromes as well as changes in the ATP/ADP ratio, and the analysis of these differences is now in progress.

*Respiratory rates at 50 % reduction of cytochrome c*

When the change in oxygen concentration as indicated by the continuous decrease in the intensity of bacterial luminescence under argon gas flow is plotted as a function of time (see Materials and Methods) the transition from zero-order to pseudo first-order kinetics is observed at oxygen concentrations in the range from 0.5 to 0.2 $\mu$M for mitochondrial respiration (cf. also refs 5 and 11). In Table I, the respiratory rates at half-maximal reduction of cytochrome *c* ($p50_c$) under several metabolic conditions are compared with the corresponding maximal rates observed under aerobic conditions. In State 4, the respiratory rate depends on whether an NADH- or a flavin-linked substrate is employed. Of particular interest is the fact that in spite of the 50 % reduction of cytochrome *c*, the respiratory rates at $p50_c$ still correspond to 70–99 % of the maximal rate. In the presence of ATP and its generating system, the maximal respiration and the respiration at $p50_c$ are depressed, the latter

TABLE I

THE COMPARISON OF RESPIRATORY RATES AT $p50_c$ WITH THEIR MAXIMAL RATES UNDER VARIOUS METABOLIC CONDITIONS

The respiratory rates were measured as described in Materials and Methods. The reaction mixture used was 'high chloride' medium. The concentrations of substrates used were: succinate, glutamate and malate, each 6 mM; $\beta$-hydroxybutyrate, 2 mM; malonate, 1.6 mM. ADP (0.5 mM) and ATP (0.5 mM) were used with their generating systems, respectively, as described for Figs 3 and 5. Mean value of three mitochondrial preparations is given in this table.

| Substrate and condition | $V$ (nmoles $O_2$/min per mg) | $p50_c$ ($\mu$M) | $V_{at\ p50_c}$ (nmoles $O_2$/min per mg) | $\frac{V_{at\ p50_c}}{V} \times 100\ \%$ |
|---|---|---|---|---|
| Succinate+glutamate +malate | 48 | 0.23 | 45 | 93 |
| Succinate+glutamate | 47 | 0.23 | 46 | 99 |
| Glutamate | 20 | 0.10 | 15 | 74 |
| $\beta$-Hydroxybutyrate | 15 | 0.12 | 14 | 91 |
| Endogeneous substrates | 5 | 0.035 | 4 | 76 |
| Succinate+glutamate +ADP | 173 | 0.27 | 45 | 26 |
| Succinate+glutamate +ATP | 32 | 0.15 | 21 | 65 |
| Succinate+glutamate +malonate | 21 | 0.14 | 11 | 54 |

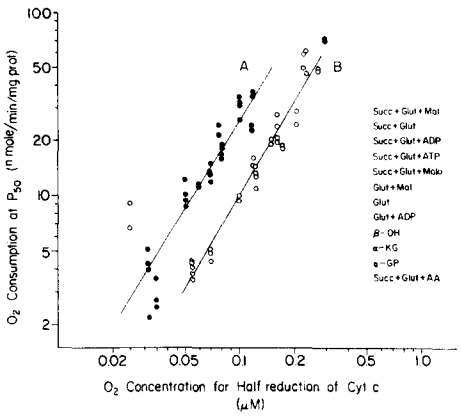


Fig. 6. The relationship between the oxygen concentration for half-maximal reduction of cytochrome *c* ($p50_c$) and the rate of oxygen consumption at $p50_c$. A, "high phosphate" medium; B, "high chloride" medium; other conditions as in Fig. 4. Oxygen consumption was measured as described in the text. Twelve different conditions were employed, as indicated in the figure. The generating system for maintaining the ATP level consisted of 0.5 mM ATP, 3 mM phosphoenolpyruvate, pyruvate kinase (5 mg of protein) and 2 mM $MgCl_2$. Suc, succinate; Glut, glutamate; Mal, malate; Malo, malonate; β-OH, β-hydroxybutyrate; α-GP, α-glycerophosphate; AA, antimycin A.

corresponding to 65 % of the former. The respiration is also restricted by the availability of phosphate acceptor and hence the presence of ADP and inorganic phosphate markedly accelerate the respiration; thus, respiration at $p50_c$ in the presence of ADP and its generating system is only 26 % of the maximum under these conditions but the absolute rate is close to that observed without ADP at $p50_c$.

In Fig. 6, the $p50_c$ values observed under various conditions are plotted as a function of the respiratory rate at each $p50_c$ in double logarithmic coordinates. These experiments were carried out in "high phosphate" and "high chloride" media. A high phosphate concentration shifts the linear plot towards low oxygen concentrations; the slope is approx. 1.4, i.e. the respiratory rate at $p50_c$ is proportional to $[O_2]^{1.4}$. It is obvious that at half-maximal reduction of cytochrome *c* the respiratory rate is a function of the corresponding oxygen concentration. The data also indicate that $p50_c$ is related to the rate of mitochondrial respiration, whether determined by the nature of the substrate or of the energy-coupling system.

*Effect of oxygen on the energy-dependent reduction of pyridine nucleotide in the presence of succinate*

Succinate-linked pyridine nucleotide reduction [16] has been re-examined as a factor indicative of the oxygen requirement for energy coupling. In the course of these studies, the end-point of pyridine nucleotide reduction in the presence of succinate was compared with that in the presence of glutamate, with and without supplements of EDTA. As shown in Fig. 7, the pyridine nucleotides are more reduced with glutamate in the absence than in the presence of EDTA; however the level of reduction obtained with succinate following glutamate is identical in both systems. The EDTA effect is, as might be expected, eliminated by the addition of magnesium (0.8–3 mM) or calcium (0.2–0.7 mM). In order to maximize the extent of pyridine

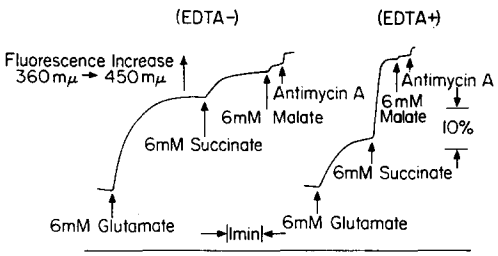


Fig. 7. The effect of EDTA on glutamate- and succinate-linked pyridine nucleotide reduction. 15 mg of pigeon heart mitochondrial protein suspended in 30 ml of a reaction medium containing 0.225 M mannitol, 0.075 M sucrose, 2 mM $K_2PO_4$, and 20 mM trismorpholinopropanesulfonic acid (pH 7.2). 0.2 mM EDTA and 15 $\mu$g antimycin A as indicated.

nucleotide reduction by succinate, 0.2 mM EDTA was added in the experiment described below.

Fig. 8 shows the oxygen dependence of cytochrome *c* and pyridine nucleotide reduction. Initially, glutamate and succinate are added under aerobic conditions, and cause corresponding reductions in both cytochrome *c* and pyridine nucleotides. In anaerobiosis, cytochrome *c* is further reduced but pyridine nucleotide becomes slowly oxidized [17]. Thereafter, the oxygen concentration is increased in a stepwise fashion and causes stepwise oxidation of cytochrome *c*. Pyridine nucleotides are initially oxidized and then, as the oxygen concentration increases they become more reduced, the extent of the oxygen-induced reduction exceeding that observed in anaerobiosis. The phenomenon reverses in a similar way; decreases in oxygen concentration from the aerobic state produce first an oxidation of pyridine nucleotide and then a slight increase of reduction.

Fig. 9 illustrates the properties of the system with a supplement of glutamate in the presence of 0.2 mM EDTA. Half a minute after cytochrome *c* reduction is registered, maximal reduction of pyridine nucleotide occurs. Titration with oxygen at this point causes a sensitive response of the pyridine nucleotides: when an oxygen concentration at which further reduction might be expected is reached, a plateau is

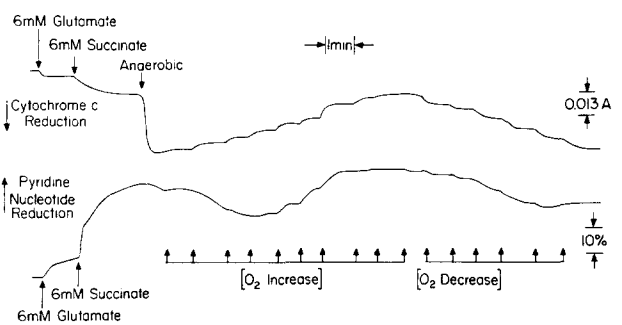


Fig. 8. Effect of oxygen concentration on the redox state of cytochrome *c* and pyridine nucleotides. "Standard" reaction medium as described in Fig. 7. The arrows "$O_2$ increase" and "$O_2$ decrease" indicate the points at which the oxygen concentration in the gas flow was increased or decreased in stepwise fashion, respectively.

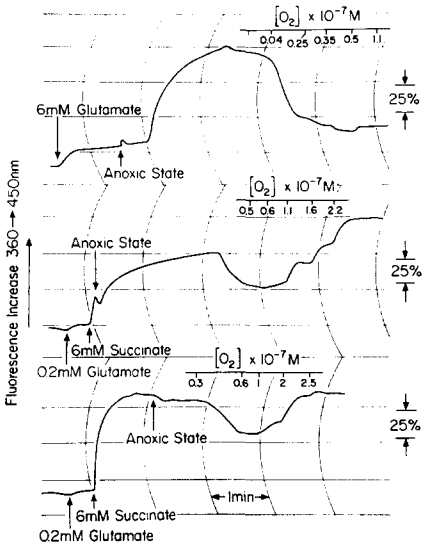


Fig. 9. Differences in the extent of pyridine nucleotide reduction induced by succinate addition and by anaerobiosis. The experimental conditions were as described in Fig. 8. The times of succinate addition are indicated in the figure. The oxygen concentration at each steady state was estimated from the redox state of cytochrome *c*, measured simultaneously.

seen instead. Apparently, the endogenous succinate generated from glutamate oxidation by transamination and subsequent reactions may be just sufficient to maintain the trace horizontal as the oxygen concentration increases. In the middle trace, an addition of succinate to the glutamate-supplemented system is made just before the reduction of cytochrome *c* begins. Thus, both aerobic succinate-dependent and endogenous energy stores are available to cause an initial immediate and subsequent slow reduction of pyridine nucleotides. The extent of the reduction, however, is

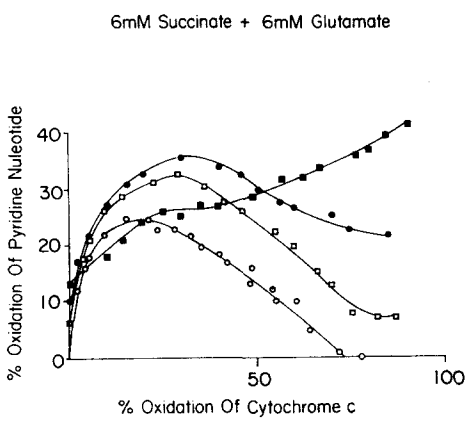


Fig. 10. The effect of malonate concentration on the oxygen-dependent reduction of pyridine nucleotide in the presence of succinate. Experimental conditions as in Fig. 8. ○, without malonate; □, 0.4 mM malonate; ●, 0.8 mM malonate; ■, 1.6 mM malonate.

limited as compared with that observed in Fig. 8. When, as in the bottom trace, glutamate and succinate are metabolized for a significant interval prior to anaerobiosis, the level of reduction obtained in the anoxic state is slightly lower than that obtained in the aerobic state.

Further evidence for the oxygen dependence of pyridine nucleotide reduction by succinate is afforded by the observation that uncouplers, ADP, or $Ca^{2+}$ (300 $\mu$M) abolish the phenomenon shown in Figs 8 and 9. Similarly, malonate causes inhibition of the reduction, with half-maximal effect being obtained with 1.6 mM malonate at 6 mM succinate, as shown in Fig. 10.

The phenomenon of oxygen-dependent reduction of pyridine nucleotides described above may be considered to be a reflection of the steady-state level of the energy store in the respiratory system as a balance of the rates of energy production and energy utilization, although the oxidation level of pyridine nucleotides, once attained with succinate under aerobic conditions, is not so quickly lowered as might be expected for the loss of energy store due to anaerobiosis.

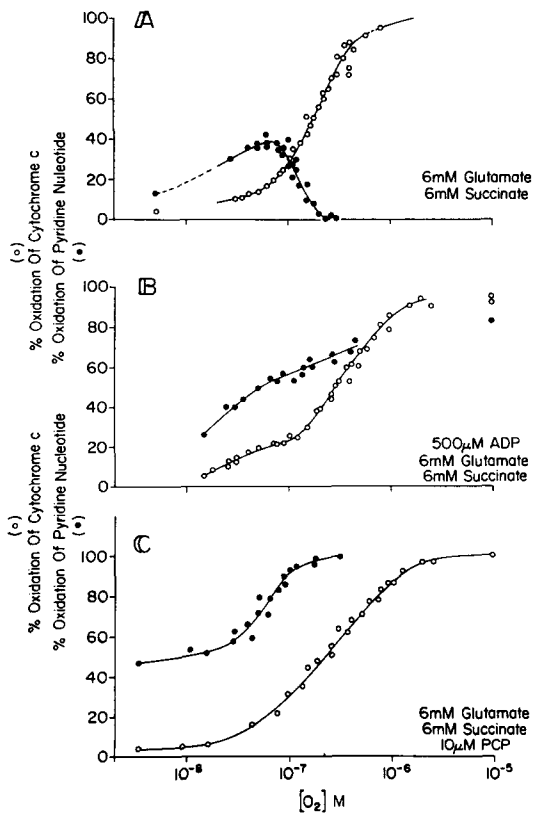


Fig. 11. The effect of oxygen concentration on the redox states of cytochrome *c* and pyridine nucleotide in State 3, State 4, and the uncoupled state. Experimental conditions as in Fig. 8. The oxygen concentrations were estimated according to the data of Fig. 4. Top trace, State 4; middle trace, State 3; bottom trace, uncoupled with pentachlorophenol.

*Oxygen concentration and the redox state of pyridine nucleotides*

In order to identify the oxygen requirement for half-maximal pyridine nucleotide reduction, termed $p50_{PN}$, the oxidation–reduction levels of pyridine nucleotides are compared with those of cytochrome *c* as a function of oxygen concentration under various metabolic conditions in Fig. 11. In State 4, with succinate and glutamate, the transition from oxygen-dependent oxidation to reduction occurs at 0.09 $\mu$M oxygen. In the presence of 500 $\mu$M ADP with its generating system, half-maximal reduction of pyridine nucleotides is observed at an oxygen concentration of approximately 0.08 $\mu$M, with no oxygen-induced reduction phenomenon. With uncoupled mitochondria, the maximal reduction of pyridine nucleotides by glutamate and succinate is only 55 % of the succinate-induced reduction under aerobic conditions; under these conditions, $p50_{PN}$ apparently occurs when the oxygen concentration decreases to about 0.06 $\mu$M. This figure also shows that the oxygen requirement for cytochrome *c* reduction varies significantly in the different metabolic states, while that for pyridine nucleotide reduction does not.

*Effects of oligomycin and ruthenium red on the oxygen-induced reduction of pyridine nucleotides*

The formation of a high-energy intermediate during mitochondrial respiration has been postulated (cf. refs 18 and 19); this intermediate is then utilized for ATP synthesis, ion transport, energy-dependent pyridine nucleotide reduction, and other energy-linked reactions. Therefore, the steady-state concentration of the high-energy intermediate (or the chemical potential available for energy production) may depend upon a balance of the respiratory rate and the rate of energy utilization. The oxygen-induced reduction of pyridine nucleotides by succinate may be used as a parameter proportional to the steady-state concentration of the high-energy intermediate. Similar considerations apply in the case of a chemi-osmotic hypothesis (cf. refs 18 and 19).

The effects of oligomycin and ruthenium red, which are inhibitors of oxidative phosphorylation and $Ca^{2+}$ transport, respectively, on the minimum oxygen concentration required for the oxygen-induced reduction of pyridine nucleotides have

TABLE II

REDOX STATE OF CYTOCHROME *c* AT WHICH THE OXYGEN-DEPENDENT NAD REDUCTION IS ABOLISHED

The experimental conditions were as described for Fig. 7, except that 0.2 mM EDTA was present. Mean values of 2–5 separate experiments are given.

| Additions | Percent reduction of cytochrome *c* | Oxygen ($\mu$M) |
|---|---|---|
| Succinate + glutamate | 72 | 0.09 |
| + oligomycin (0.5 $\mu$g/ml) | 83 | 0.06 |
| + ruthenium red (0.05 $\mu$g/ml) | 80 | 0.07 |
| + ruthenium red (0.1 $\mu$g/ml) | 85 | 0.05 |
| + oligomycin (0.5 $\mu$g/ml) and ruthenium red (0.1 $\mu$g/ml) | 90 | 0.03 |
| + ATP and generating system | 85 | 0.05 |

been examined, and the results are reported in Table II. Under State 4 conditions, the oxygen-induced reduction is observed at an oxygen concentration of 0.09 $\mu$M. This minimum oxygen concentration decreases further as the inhibition of $Ca^{2+}$ transport by ruthenium red increases, and oligomycin causes a similar effect; the oligomycin and ruthenium red effects appear to be additive. Of particular interest is the case in the presence of ATP and its generating system; the maximal extent of pyridine nucleotide reduction achieved under aerobic conditions decreases with decreasing oxygen, down to a concentration of 0.03 $\mu$M. This phenomenon may be due to the inability of the ATP-generating system to maintain the mitochondria in a true energy-rich state under hypoxic conditions; alternatively, it may be possible that the internally-generated energy state is more potent than that which can be achieved with added ATP.

*The effect of oxygen concentration on mitochondrial $Ca^{2+}$ uptake*

The jellyfish protein, aequorin, interacts with $Ca^{2+}$ to form a complex which exhibits bioluminescence with a half-time of 270 $\mu$s [14]. $Ca^{2+}$ release from mitochondria can thus be measured by following the appearance of the aequorin–$Ca^{2+}$ luminescence. In Fig. 12A, the redox state of cytochrome *c* and the rate of $Ca^{2+}$ efflux are measured simultaneously under various oxygen concentrations. Under aerobic conditions, the addition of 2 nM aequorin does not produce significant luminescence (the slight increase in the luminescence intensity trace is probably due to a change in light scattering), indicating that the endogenous $Ca^{2+}$ has already

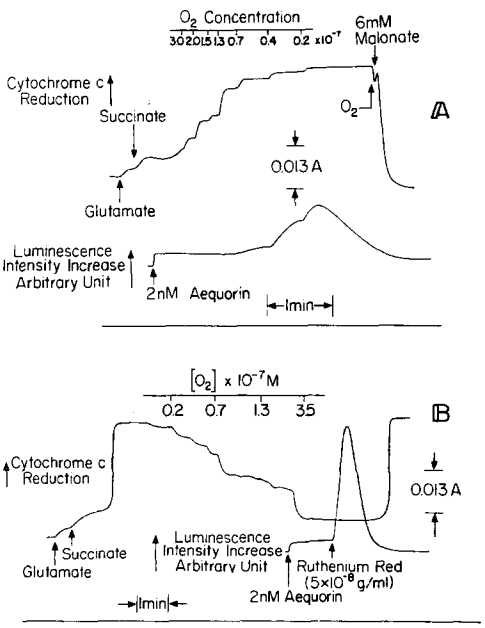


Fig. 12. The relation between the redox state of cytochrome *c* and $Ca^{2+}$ release from mitochondria. Experimental methods and materials as described in the accompanying text. The steady-state oxygen concentration was estimated from the redox state of cytochrome *c* as calibrated by *Ph. phosphoreum* under similar conditions. 30 mg of pigeon heart mitochondrial protein.

TABLE III

THE MINIMUM OXYGEN CONCENTRATION PRODUCING $Ca^{2+}$ RELEASE FROM MITOCHONDRIA UNDER VARIOUS METABOLIC CONDITIONS

The method of $Ca^{2+}$ determination, utilizing aequorin, was as described in Materials and Methods. The concentration of substrate used was 6 mM, except that β-hydroxybutyrate concentration was 2 mM. Oligomycin (0.5 μg/ml) was added to the reaction medium under anaerobic condition. Mean values of the results in 2–7 separate experiments given in this table.

| Additions | Minimum $O_2$ concentration (μM) | Percent reduction of cytochrome *c* |
|---|---|---|
| Succinate+glutamate+malate | 0.10 | 66 |
| Succinate+glutamate | 0.09 | 70 |
| Glutamate+malate | 0.11 | 58 |
| Glutamate | 0.06 | 47 |
| β-Hydroxybutyrate | 0.09 | 41 |
| Succinate+glutamate+ADP | 0.5 | 38 |
| Succinate+glutamate+oligomycin | $< 0.01$ | $\approx 100$ |

been taken up by the mitochondria. Thereafter, decreases in the oxygen concentration from 0.3 to 0.07 μM, as indicated by the corresponding reduction of cytochrome *c*, do not cause any aequorin–$Ca^{2+}$ luminescence. When cytochrome *c* approaches 70 % reduction, which corresponds to an oxygen concentration of approx. 0.04 μM under these conditions, the aequorin–$Ca^{2+}$ complex begins to form, as indicated by the appearance of luminescence. Since the slope of the luminescence trace is proportional to the rate of $Ca^{2+}$ efflux from the mitochondria, it is obvious that the rate of $Ca^{2+}$ efflux, which is the sum of the rate of passive efflux and active influx, accelerates as the oxygen concentration decreases. The maximal rate of $Ca^{2+}$ efflux as determined by this method is shown in Fig. 12B, in which addition of ruthenium red under aerobic conditions produces an instant release of $Ca^{2+}$ and consequently, the appearance of luminescence.

Since the exact calibration of the aequorin data is difficult, values for half-maximal release of $Ca^{2+}$ are not employed here. Instead, the oxygen concentrations at which $Ca^{2+}$ release is first observed, being more accessible, are summarized in Table III. In State 4 conditions, oxygen concentrations of 0.1–0.04 μM are obtained with various substrates. In State 3, $Ca^{2+}$ release is observed already at 0.5 μM oxygen. In the presence of oligomycin, no $Ca^{2+}$ release is observed until the oxygen concentration is below 0.01 μM. Of particular interest is the fact that $Ca^{2+}$ release begins to be observed only after the energy-dependent reduction of pyridine nucleotide has been abolished.

## DISCUSSION

Studies on the respiration of biological systems [2–4, 8, 9, 20] and on the redox states of cytochromes [2, 5, 21] as a function of oxygen concentration have been carried out mainly by using the sensitive polarographic method and by analyzing the transition from zero- to first-order kinetics in an aerobic–anaerobic transition. As Lübbers [6], as well as Degn and Wohlrab [21], have recently pointed out, this

approach is limited in sensitivity and there are complexities of the electrode phenomena which may give an early break in the curve or an error in the indication of zero oxygen. Notwithstanding these problems at low oxygen concentrations, the stationary or vibrating platinum microelectrode is most useful for determining steady-state oxygen utilization rates [22].

An alternative method for low oxygen concentrations is the technique of bacterial luminescence which was first applied by Schindler [5, 2] to the analysis of the kinetics of the oxygen reaction in cytochrome oxidase of yeast cells and pigeon heart mitochondria. In that paper [2], the interest was mainly in determining whether or not there was reversibility in the reaction of cytochrome oxidase with oxygen, and also the velocity constant for this reaction. In the work reported here, the emphasis has been placed upon the oxygen requirement for electron transport and energy coupling in mitochondria in different steady-state metabolic conditions. The possibility that an oxygen gradient across the mitochondrion interfered with the exact determination of the oxygen requirement is rendered unlikely by diffusion calculations. The oxygen affinities of yeast hemoglobin within the yeast cell and that in the isolated, purified state, as well as the velocity constants for the reaction of cytochrome $a_3$ of intact ascites tumor cells and mitochondria isolated from them [23], were found to be identical.

In support of the equations derived previously for the oxygen affinity of the respiratory chain [2], it was found that the oxygen concentration required to provide 50 % oxidation of cytochrome *c* ($p50_c$) depends approximately linearly upon the rate of respiration as influenced by the electron flow rate (substrate) and the energy-coupling reactions (State 3, State 4, and the uncoupled state) as shown in Fig. 6. The values for $p50_c$ and $p50_{PN}$ determined in this study may be of great importance in calibrating the tissue oxygen tension in organs such as liver, heart, and brain in which the redox states of cytochrome *c* and/or pyridine nucleotide can be measured by spectrophotometry [24] or surface fluorimetry [25]. Although pigeon heart mitochondria were used in this study, an almost identical value of $p50_{PN}$ has been obtained with rat brain mitochondria [26].

The choice of cytochrome *c* as the reference cytochrome is justified by the very slight effect of the phosphate potential upon its midpoint [27] and by its rapid equilibration with cytochromes $c_1$ and *a* [28]. One might prefer to use cytochrome oxidase as the reference pigment since it is directly involved in the reaction with oxygen and has indeed been so employed in previous studies, particularly those with Chance et al. [23]. In view of the subsequent finding that the mid-potential of cytochrome $a_3$ is highly ATP dependent [29], we now prefer to use cytochrome *c*. Also, the overlapping of the absorption bands of cytochromes *a* and $a_3$ in the region of the $\alpha$ and $\gamma$ bands [29] renders cytochrome *a* less suitable than cytochrome *c* as a reference cytochrome, and requires further study.

Fig. 6 also illustrates the proportionality between the $p50_c$ and the respiratory rate. In State 4, the respiratory rate observed at $p50_c$ is very close to the maximum, while in State 3 it is only one-fourth the maximum, since the respiratory rate is controlled by the phosphate potential and the substrate potential, as well as by the oxygen concentration. This is, in principle, in agreement with other observations that the rate of mitochondrial ATP synthesis in State 3 falls to half at an oxygen concentration of 2.5 $\mu$M, whereas in State 4 the oxygen concentration for half-maximal ATP

synthesis is 0.3 $\mu$M (cf. Fig. 4 of ref. 2). Those values were determined by the oxygen electrode and are too large by a factor of approx. 3. The present results give values of apparent $K_m$ that are also dependent upon the metabolic state but are numerically smaller.

The question arises, "What do the terms 'critical oxygen concentration' or 'apparent $K_m$ of oxygen' for cell respiration mean?". As discussed previously [2], the $K_m$ value for mitochondrial respiration can be expressed approximately as $V/k_1 e$, where $k_1$ and $e$ are the rate constant for the reaction of cytochrome $a_3$ with oxygen and the concentration of cytochrome $a_3$, respectively. $V$ depends upon the substrate activity and on the phosphate potential [ATP]/[ADP][$P_i$] as mentioned above. Thus, the 'critical oxygen concentration' may not directly reflect the intrinsic characteristics of tissue respiration itself, but rather those of the energy metabolism of the tissue as a consequence of the balance between energy production and energy utilization.

The interpretation of tissue anoxia based upon pyridine nucleotide fluorescence requires a knowledge of whether or not the succinate-linked pathway is operative. Direct observations in tissues indicate that the degree of pyridine nucleotide reduction increases monotonically in the normoxic–anoxic transition [10, 30]; titrations similar to those of Fig. 8 in the presence of succinate are not observed. Presumably, the NAD-linked substrates of the citric acid cycle are in adequate supply as compared with electron flow from succinate, and the phosphate potential is sufficiently low that titration curves of the type shown in Fig. 9 (top) and Fig. 10 (middle) are characteristic of the functioning tissue, while those of Fig. 8 are not. Thus, one may with confidence identify that at concentrations of 0.01 $\mu$M oxygen and greater, the pyridine nucleotides will be substantially oxidized and the $p50_{PN}$ can be used in a semi-quantitative fashion to measure the tissue oxygen concentration in the region from 0.01 to 0.1 $\mu$M (0.007–0.07 Torr).

The simplest procedure for determining the metabolic state corresponding to a given $p50_{PN}$ involves a consideration of the characteristics of the organ itself. For example, resting skeletal muscle [31] would be expected to have a State 4 electron flow rate, while the same tissue in active contraction would have a State 3 rate. Similarly, cardiac tissue would be expected to be near State 3, and observations of blood flow and oxygen extraction on the brain cortex [10] indicate that a similar situation exists there. Biochemical determinations [32, 33] indicate that the metabolic state of the liver is between State 3 and State 4. Similar considerations apply to all the organs. In other words, an inspired oxygen concentration giving half-maximal pyridine nucleotide reduction is experimentally determined for the organ in situ and the $p50_{PN}$ is selected from in vitro studies for the appropriate metabolic state of the organ.

An alternative approach, more difficult from the experimental point of view, is to determine the NADH oxidation–reduction level of the tissue corresponding to States 2, 3, 4, and 5. The metabolic state of the tissue is then identified by comparing the redox state of the tissue pyridine nucleotide with these predetermined values; the appropriate $p50_{PN}$ for this metabolic state is then known from the in vitro data. Such a range of metabolic states in tissue could be obtained by local perfusion with appropriate substrates and inhibitors, or by subjecting the whole animal to the metabolic extremes demanded by the State 2–4 transitions.

A third possibility depends upon a quantitation of the NADH fluorescence in terms of the actual NADH content of the tissue. In this way, the fluorescence of NADH obtained in a particular metabolic state could be compared with the analytical data for the tissue and the metabolic rate thereby determined.

While we are at present far from the ideal of having these three approaches available, it would seem appropriate to employ the $p50_{PN}$ obtained in State 3 for heart and brain, and in State 4 for liver, as first approximations to the $p50_{PN}$ for these tissues in vivo.

ACKNOWLEDGEMENTS

The authors wish to thank Dr R. Oshino for advice and helpful discussion on the oxygen assay.

This research was supported by U.S.P.H.S. GM 12202, NDS 10939, HD 06274 and AA 00292.

REFERENCES

1 Caster, R. E. (1964) in Oxygen in the Animal Organism (Dickens, F. and Neil, E., eds), pp. 239–246, Pergamon Press, Oxford
2 Chance, B. (1965) J. Gen. Physiol. 49, 163–188
3 Wittenberg, J. B. (1970) Physiol. Rev. 559–634
4 Chance, B. (1957) Fed. Proc. 16, 671–680
5 Schindler, F. (1964) Ph. D. thesis, University of Pennsylvania
6 Lübbers, D. W. (1968) in Oxygen Transport in Blood and Tissues (Lübbers, D. W., Luft, U. C., Thews, G. and Witzlels, E., eds), pp. 124–139, Thieme, Stuttgart
7 Oshino, R., Oshino, N., Chance, B. and Hagihara, B. (1973) Eur. J. Biochem. 35, 23–33
8 Baender, A. and Kiesse, M. (1955) Arch. Exp. Pathol. Pharmakol. 224, 312–321
9 Longmuir, I. S. (1957) Biochem. J. 65, 378–382
10 Chance, B. and Schoener, B. (1962) Nature 195, 956–958
11 Schindler, (1967) Methods Enzymol. 10, 629–634
12 Oshino, R., Oshino, N., Tamura, M., Kobilinsky, L. and Chance, B. (1972) Biochim. Biophys. Acta 273, 5–17
13 Chance, B., Mayer, D. and Rossini, L. (1970) IEEE Trans. BME-17, 118–121
14 Shimomura, O., Johnson, F. H. and Saiga, Y. (1962) J. Cell. Comp. Physiol. 59, 223–239
15 Chance, B. and Hagihara, B. (1963) Proc. 5th Int. Congr. Biochem. Vol. V, pp. 3–37, Pergamon Press, Oxford
16 Chance, B. and Hollunger, G. (1961) J. Biol. Chem. 236, 1534–1543
17 Chance, B. and Hollunger, G. (1961) J. Biol. Chem. 236, 1562–1568
18 Greville, G. D. (1969) Curr. Top. Bioenerg. 3, 1–78
19 Slater, E. C. (1971) Q. Rev. Biophys. 4, 35–71
20 Winzler, R. J. (1941) J. Cell. Comp. Physiol. 17, 263–276
21 Degn, H. and Wohlrab, H. (1971) Biochim. Biophys. Acta 245, 347–355
22 Chance, B. and Williams, G. R. (1956) Adv. Enzymol. 17, 65–134
23 Chance, B., Schoener, B. and Schindler, F. (1964) in Oxygen in the Animal Organism (Dickens, F. and Neil, E., eds), pp. 367–392, Pergamon Press, Oxford
24 Scholz, R. and Bücher, Th. (1965) in Control of Energy Metabolism (Chance, B., Estabrook, R. W. and Williamson, J. R., eds), pp. 393–413, Academic Press, New York
25 Chance, B., Salkovitz, I. and Kovach, A. G. B. (1972) Am. J. Physiol. 223, 207–218
26 Chance, B., Oshino, N., Sugano, T. and Mayevsky, A. (1973) Adv. Exp. Med. and Biol. 37A, pp. 277–292, Plenum Publishing, New York
27 Dutton, P. L., Wilson, D. F. and Lee, C. P. (1970) Biochemistry 9, 5077–5082
28 Chance, B. and Pring, M. (1969) Colloq. Ges. Biol. Chem. 18, 102–126

29 Lindsay, J. G. and Wilson, D. F. (1972) Biochemistry 11, 4613–4621
30 Chance, B. and Schoener, B. (1965) Biochem. Z. 341, 340–345
31 Chance, B., Mauriello, G. and Aubert, M. (1962) in Muscle as a Tissue (Rodahl, K. and Horvath, S., eds), pp. 128–145, McGraw-Hill, New York
32 Williamson, J. R., Scholz, R., Browning, E. T., Thurman, R. G. and Fukami, M. H. (1969) J. Biol. Chem. 244, 5044–5054
33 Brauser, B., Bücher, Th., Sies, H. and Versmold, H. (1972) in Molecular Basis of Biological Activity (Gaede, B. K., Horecker, B. L. and Whelan, W. J., eds), pp. 197–219, Academic Press, New York